Journal of Materials Chemistry B

PAPER

View Article Online
View Journal | View Issue

Cite this: J. Mater. Chem. B, 2014, 2, 7459

NIR fluorescence labelled carbon nano-onions: synthesis, analysis and cellular imaging†

Silvia Giordani,*[a] Juergen Bartelmess,[a] Marco Frasconi,[a] Ilaria Biondi,[bc] Shane Cheung,[bc] Marco Grossi,[bc] Dan Wu,[bc] Luis Echegoyen[d] and Donal F. O'Shea*[bc]

Received 4th July 2014
Accepted 2nd September 2014

DOI: 10.1039/c4tb01087f

www.rsc.org/MaterialsB

The preparation of novel NIR fluorescent carbon based nanomaterials, consisting of boron difluoride azadipyrromethene fluorophores covalently attached to carbon nano-onions, is demonstrated. In addition, the analysis of the new nanomaterial is presented. The fluorescent nano-derivative properties are customized such that their emission can be reversibly on/off modulated in response to pH, which is demonstrated in solution and in cells. The *in vitro* imaging of HeLa Kyoto cells is carried out and the cellular uptake of the carbon nano-onion NIR fluorophore conjugates is verified.

Introduction

Nano-platforms capable of carrying therapeutic agents as well as producing an optical output in recognition of a specified target for imaging hold great potential in the treatment of cancer and other diseases.[1,2] Despite much interest in other carbon-based nano-materials, multi-shell fullerenes, known as carbon nano-onions (CNOs), as functional constructs for intracellular transport have not yet been explored. CNOs, discovered in 1992, are structured by concentric shells of carbon atoms,[3,4] showing several unique properties. They exhibit a graphitic multilayer structure along with a low density and a large surface area to volume ratio.[5,6]

Initial investigations of the effects of large CNOs (diameter of approximately 30 nm) on the immune system indicated that the cell response was highly dependent on the structure of the carbon nanomaterial.[7] We recently reported the weak inflammatory potential and low cytotoxicity *in vitro* and *in vivo* of small surface functionalized CNOs (diameter of approximately 5 nm) and their ability to be taken up by antigen displaying cells, demonstrating that the inflammatory properties of the CNOs can be controlled by the chemical functionalities present on their surface.[8] These promising biological results led us to investigate the development of novel intracellular imaging systems based on CNOs, with special attention to the biologically important near-infra red (NIR) region.[9] Absorption and emission in the NIR region is of great importance for applications in biology, as NIR light has dramatically lower light induced cellular toxicity than shorter wavelengths and is more effectively transmitted through body tissue. NIR fluorescence imaging is an inexpensive and non-invasive technique with potential for use in real-time.[10] In addition to our study using fluorescein labelled CNOs,[7] there are only two other reports on the use of CNOs for biological imaging: the group of Sarkar used water-soluble, defect rich, oxidized CNOs, synthesized from wood waste, for imaging the life cycle of *Drosophila melanogaster*[11] and to study *Escherichia coli* and *Caenorhabditis elegans*.[12]

Boron difluoride azadipyrromethenes are a relatively new class of NIR fluorophores with emerging biological and medicinal applications.[13–15] They are also used for molecular sensing,[16,17] as building blocks in light-harvesting systems[18–22] and they have been successfully employed for the functionalization of carbon nanotubes.[23,24]

In this study, we report first the synthesis and characterization of NIR active boron difluoride azadipyrromethene[25] functionalized CNOs and we investigate their uptake in HeLa Kyoto cells. We demonstrate that the NIR-fluorophore is able to retain emissive properties when conjugated to the CNOs and upon internalization by cells. Importantly, we report that the NIR-emission of the nanoparticles can be on/off modulated in response to pH both in solution and in the cells.

Results and discussion

Synthesis

The synthetic procedure used to prepare CNO-NIR fluorophore nanoparticles is illustrated in Scheme 1; detailed synthetic procedures can be found in the ESI.† Pristine CNOs (**p-CNO**) were covalently functionalized using the one-pot Tour reaction comprising 4-aminobenzoic acid and isoamylnitrite to produce

[a]Istituto Italiano di Tecnologia (IIT), Nano Carbon Materials, Via Morego 30, 16163 Genova, Italy. E-mail: silvia.giordani@iit.it
[b]Department of Pharmaceutical and Medicinal Chemistry, Royal College of Surgeons in Ireland, 123 St. Stephen's Green, Dublin 2, Ireland. E-mail: donalfoshea@rcsi.ie
[c]School of Chemistry and Chemical Biology, University College Dublin, Belfield, Dublin 4, Ireland
[d]Department of Chemistry, University of Texas at El Paso, El Paso, Texas, USA

† Electronic supplementary information (ESI) available: Various procedures, TGA results, additional spectroscopy and discussion. See DOI: 10.1039/c4tb01087f

benzoic acid functionalized and dispersible **CNO-CO_2H**,[26] that was then converted to the corresponding electrophilic activated ester intermediate **CNO-AE** by activation with *N*-hydroxysuccinimide. The synthesis of NHBoc-protected boron difluoride azadipyrromethene derivative Boc-**1a** was previously published[10] and Boc-**1b** was synthesized as described in the ESI.† Following Boc deprotection, amino functionalized NIR-fluorophores **1a** and **1b** reacted with **CNO-AE** in DMF at RT for 72 hours. Then, the non-covalently bound fluorophore was removed from **CNO-1a** and **CNO-1b** by repeated dispersion of the particles in DMF and centrifuged until the supernatant was no longer fluorescent.

Characterization of NIR-fluorescent CNO nanoparticles

The functionalized carbon nano-onions were characterized by a number of techniques, including thermogravimetric analysis (TGA), Raman, Fourier transform infrared (FTIR), absorption and emission spectroscopy as well as atomic force microscopy (AFM) and high resolution transmission electron microscopy (HRTEM) (Fig. 1).

The TGA analysis confirms the successful covalent functionalization of the **CNO-1a** (Fig. S1 in the ESI†). The CNO decomposition temperature in air is lowered upon covalent functionalization, a result in line with earlier studies.[8,26] An increased weight loss of **CNO-1a** at lower temperatures, between 200 °C and 400 °C, verifies the presence of additional organic functionalities, the boron difluoride azadipyrromethene fluorophore. The degree of functionalization of the CNO nanomaterial was estimated from the weight losses, as described in the literature,[27] assuming that one CNO consists of 6 graphitic shells. The TGA of **CNO-CO_2H** and **CNO-1a** performed in air shows a weight loss at 400 °C of about 10% and an additional 17%, respectively. We estimated about 55 benzoic acid functionalities per onion for **CNO-CO_2H** and approx. 21 boron difluoride azadipyrromethene molecules per CNO for **CNO-1a**. This degree of functionalization leaves some benzoic acid functionalities, about 34 units, on the surface of the CNO, providing additional water-solubility for the CNO-NIR fluorophore conjugate.

Raman spectroscopy was used to follow the progress of CNO functionalization (Fig. S6 in the ESI†) and illustrates an increase of the CNO D-band, relative to the G-band, corroborating the successful covalent functionalization. The D/G-band ratio of the **p-CNO** is about 1.23 and increases upon functionalization to 1.56 for **CNO-CO_2H** and to 1.91 for **CNO-AE**. In the Raman spectrum of **CNO-1a**, a strong background fluorescence signal is observed (Fig. S7 in the ESI†), which is caused by the emission of boron difluoride azadipyrromethene at the excitation wavelength of 632 nm.

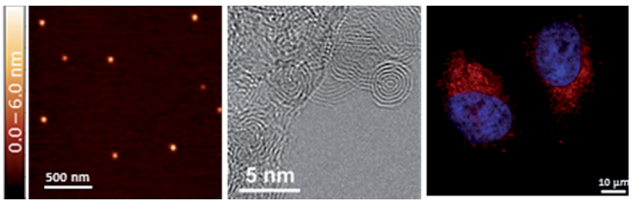

Fig. 1 AFM (left), HRTEM (centre) and confocal microscopy (right) images of **CNO-1a** (red colour), internalized in HeLa Kyoto cells in the case of the confocal microscopy image.

FTIR spectroscopy was used as an additional technique to follow the functionalization of CNOs, first with benzoic acid, which was then activated with *N*-hydroxysuccinimide (Fig. S8 in the ESI†). Also the successful subsequent functionalization with boron difluoride azadipyrromethene **1a** could be corroborated by FTIR spectroscopy (Fig. S9 in the ESI†). The IR spectrum of **CNO-1a** displays some IR bands similar to the ones found in the IR spectra of Boc-**1a**. This includes IR bands in the aromatic region at 3000 cm^{-1}. At lower wavenumbers, **CNO-1a** reveals several IR absorption bands between 600 and 1600 cm^{-1}, which can be assigned to the presence of the boron difluoride azadipyrromethene fluorophore. Some resemblance to the IR bands of **1a** is obvious, but the strong background absorption of the CNO bulk material makes it impossible to clearly identify and assign certain IR bands to specific functionalities. Nevertheless, the presence of additional IR absorption bands (when compared to those of **CNO-AE** for example), is a further indication that successful functionalization with boron difluoride azadipyrromethene fluorophores **1a** has been achieved.

The presence of the fluorophore is also evident from the absorption spectrum of **CNO-1a** (Fig. 2 – inset), where

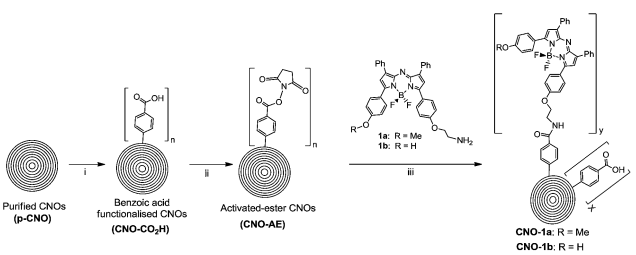

Scheme 1 (i) 4-Aminobenzoic acid, isoamyl nitrite, DMF, 60 °C, 24 h, N_2 (ii) NHS, EDC-HCl, DIPEA, DMF, RT 48 h (iii) DIPEA, DMF, RT, 72 h.

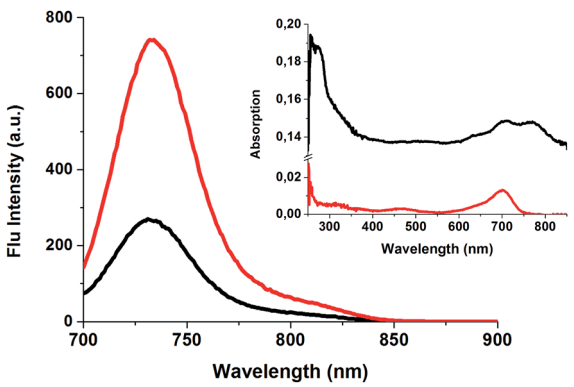

Fig. 2 Emission spectra of Boc-**1a** (red line) and **CNO-1a** (black line) that exhibit the same optical density of the fluorophore at the excitation wavelength. Inset: absorption spectra of boron difluoride azadipyrromethene derivatives Boc-**1a** (red line) and **CNO-1a** (black line). (Solvent: DMSO, λ_{exc} = 690 nm).

broadening of the boron difluoride azadipyrromethene absorption bands can be observed upon CNO functionalization. The broad background absorption observed in the absorption spectrum of **CNO-1a** is typical for nanocarbon materials.[8,23,24,26]

The boron difluoride azadipyrromethene derivatives Boc-**1a** (ref. 10) and Boc-**1b** were chosen as reference NIR fluorophores, since their molecular structure (Boc-protected amine group) is closely related to that of the CNO bound boron difluoride azadipyrromethene. The spectroscopic properties of Boc-**1a** and Boc-**1b** are summarized in detail in the ESI.†

Comparison of the fluorescence features of the boron difluoride azadipyrromethene derivatives Boc-**1a** and **CNO-1a**, at an excitation wavelength of 690 nm in DMSO, shows a reduced fluorescence intensity of the CNO conjugate while the absorption of boron difluoride azadipyrromethenes at the excitation wavelength of both samples was comparable (Fig. 2). A plausible explanation for this observation is the high background absorption of the CNOs. By comparing the maximum fluorescence intensities, the fluorescence quantum yield of **CNO-1a** was estimated to be about one third of the reference fluorophore Boc-**1a** (about 0.08 for **CNO-1a** *vs.* 0.25 for Boc-**1a**). The fluorescence lifetime of Boc-**1a** in DMSO is 2.7 ns, while upon attachment to the CNOs, the fluorescence lifetime of the NIR emission decreases slightly to 2.5 ns for **CNO-1a**. In addition, the emission maximum of **CNO-1a** is observed at 731 nm, while reference compound Boc-**1a** has a fluorescence maximum of 735 nm. This small shift further corroborates successful functionalization of CNO with boron difluoride azadipyrromethene **1a**. When comparing the observation of a reduced, but not fully quenched fluorescence emission, with previous studies of single wall-carbon nanotubes (SWNTs), functionalized with similar boron difluoride azadipyrromethene derivatives, the SWNT based systems show a much larger, almost quantitative fluorescence quenching.[23,24] In a previous study, we were able to show that this fluorescence quenching in SWNT–boron difluoride azadipyrromethene conjugates was due to electron transfer from the photo-excited NIR fluorophore to the SWNTs.[23] However, in the present system, the reduction of the fluorescence emission is attributed to the strong absorption of CNO and not to other photophysical effects. The near quantitative fluorescence quenching of fluorophores covalently linked to carbon nanomaterials is a widespread problem and greatly restricts the use of these hybrid materials for biological applications.[28–30] Fortunately, this problem is dramatically reduced in these new CNO based nanomaterials. This is one of the key important aspects of the present work.

The modulation of NIR fluorescence in response to pH for the previously unreported phenolic substituted Boc-**1b** was clearly observable upon titration from pH 6.0 to 9.0 (Fig. 3). In the lower physiological pH range the phenolic fluorescence switch controller is protonated resulting in a high intensity NIR emission but upon deprotonation to the phenolate at higher pH the emission is virtually quenched completely. These titration results showed a highly efficient on/off switching for Boc-**1b** with a fluorescence enhancement factor (FEF) of >30 and an apparent pK_a of 7.3. It would be remarkable if this molecular on/off switching mechanism controlled by the phenol/phenolate inter-conversion could be maintained after its covalent linkage to the CNO (Fig. 4A).

The switching ability of the **CNO-1b** was investigated by monitoring changes in the emission upon alteration between phenol and phenolate states in DMSO by the addition of trifluoroacetic acid (TFA) or 1,8-diazabicyclo[5.4.0]undec-7-ene (DBU), respectively. The emission spectra shown in Fig. 4B clearly demonstrate the switching, where the characteristic fluorophore emission band is evident (red line) and disappears immediately upon addition of DBU base (blue line), indicating almost quantitative quenching of the excited state. The on/off switching of the excited state of **CNO-1b** is completely

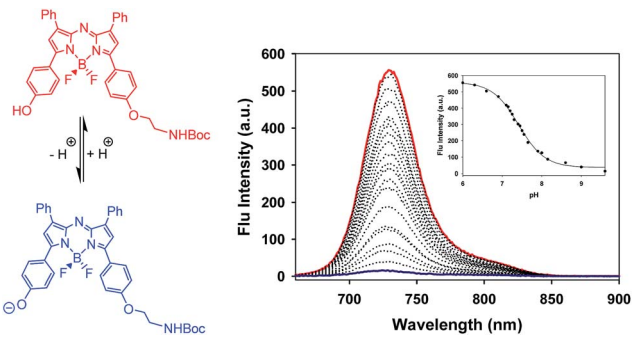

Fig. 3 Emission spectral changes for Boc-**1b** between pH 6.0 (red line) and 9.6 (blue line) at 1×10^{-7} M in water/CrEL. $I_{NaCl} = 150$ mmol L^{-1}.

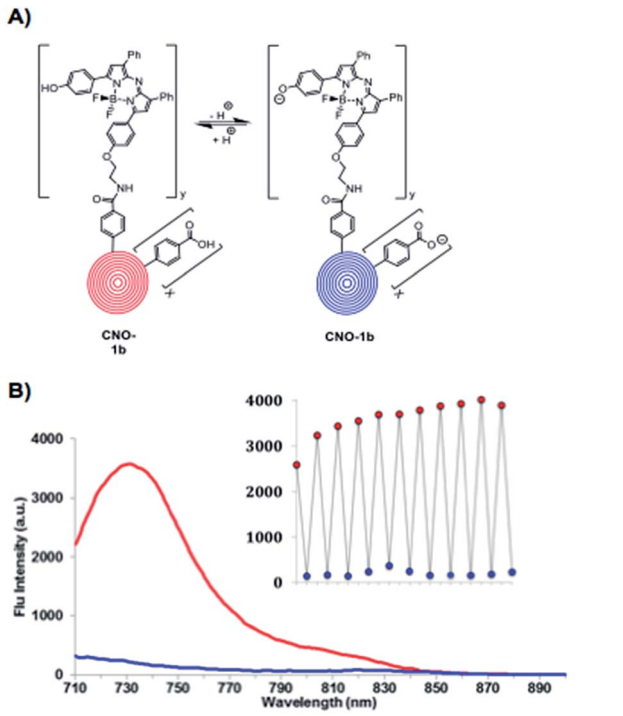

Fig. 4 (A) Schematic representation of "on"/"off" switching of **CNO-1b**. (B) Emission spectra of **CNO-1b** when protonated (red line) and deprotonated (blue line). Inset: modulation of **CNO-1b** emission at 729 nm with addition cycles of TFA and DBU (0.1 mg mL^{-1} in DMSO; $\lambda_{exc} = 690$ nm).

reversible, where modulation or cycling of the emission band at 729 nm, following repeat additions of aqueous acid (TFA) and base (DBU), is shown in the inset.

Cytotoxicity studies

In order to study the suitability of the fluorescent CNOs for cellular imaging, the cytotoxicity of the modified CNOs was tested on HeLa cells. Previous *in vitro* and *in vivo* studies of surface functionalized CNOs showed weak inflammatory properties and low cytotoxicity of CNOs.[8] In the current study, cells were treated with **CNO-CO_2H**, **CNO-AE**, **CNO-1a** and **CNO-1b** at various concentrations. Time dependence viability of the treated cells was quantified by using a resazurin-based assay, PrestoBlue™ (see ESI† for experimental details). Cells treated with only cell culture media were used as a control, and the CNO samples were compared to this control.

Cell viability is not significantly affected by **CNO-1a** up to concentrations of at least 100 μg mL^{-1} for 72 h of incubation (Fig. 5). A similar non-toxic behaviour was observed for the other fluorophore modified CNOs, **CNO-1b**, and the benzoic acid functionalized CNOs, **CNO-CO_2H**, while a significant reduction of the cell viability was detected for **CNO-AE** at 100 μg mL^{-1}.

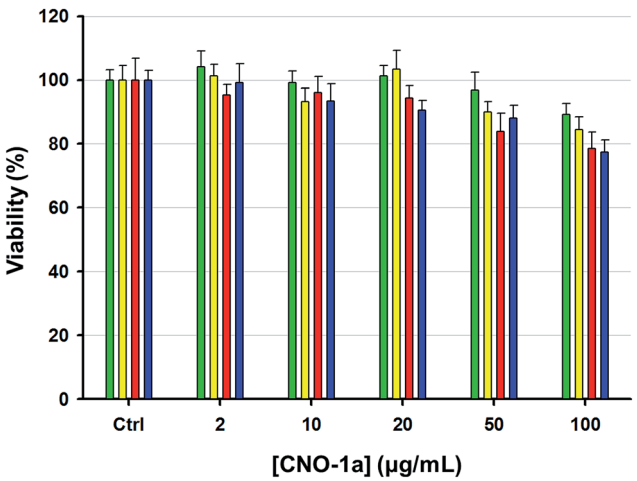

Fig. 5 Viability of HeLa cells 12 h (green bar), 24 h (yellow bar), 48 h (red bar) and 72 h (blue bar) after exposure to increasing doses (2; 10; 20; 50; 100 μg mL^{-1}) of **CNO-1a**. Viability of the treated cells is expressed relative to non-treated control cells, as the mean and the standard error of the mean of three experiments.

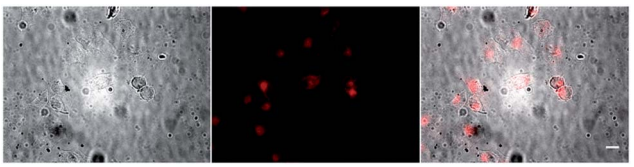

Fig. 6 Phase contrast image of HeLa Kyoto cells incubated with **CNO-1a** (left), fluorescence image of the same field of view using a Cy5 filter (middle) and phase contrast/fluorescence overlay (right) 50 μg mL^{-1} of DMSO **CNO-1a** in DMEM. All images acquired at 63×. (Scale bar 10 μm).

Collectively these results demonstrate that the chemical surface functionalization of the carbon nanomaterial largely reduces the toxicity of the CNOs. The observed high viability of the HeLa cells treated with the investigated nanomaterials allows safe use of the fluorophore functionalized CNOs as imaging agents.

Cell imaging

HeLa cells were incubated at 37 °C with **CNO-1a** for 2 hours, washed, fixed with paraformaldehyde and imaged using laser scanning confocal microscopy (LSCM). Fig. 6 illustrates that **CNO-1a** has been internalised by HeLa Kyoto cells, as a clear NIR fluorescence is observed with emission being more intense in the perinuclear region, which suggests that the CNOs are internalised by endocytosis and trafficked by lysosomes.

In order to confirm that the particles were internalised by the cells and not just localized on the plasma membrane, cell nuclei were stained blue with Hoechst 33342 and optical sectioning of the cells by laser scanning confocal microscopy (LSCM) was performed. Acquiring a *z*-stack by optical sectioning adds a third dimension of analysis, which proves that the fluorescent CNOs are distributed throughout the cytosol (Fig. 7).

To illustrate the pH response of **CNO-1b** *in vitro*, HeLa cells were incubated with a **CNO-1b** dispersion (50 μg mL^{-1}) in DMEM for two hours and fixed. After fixing, the cells were imaged and it was observed that **CNO-1b** had been successfully internalised by the cells and, as expected, were fluorescent at a physiological pH. To determine if the pH responsive **CNO-1b**

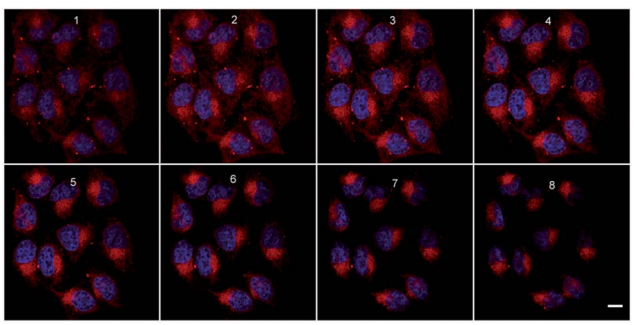

Fig. 7 Eight optical slices of HeLa Kyoto cells incubated with **CNO-1a**, taken through the *z*-axis. Images 1–8 from the bottom of the cell to the top. Nuclei stained blue with Hoechst 33342. (Scale bar 10 μm).

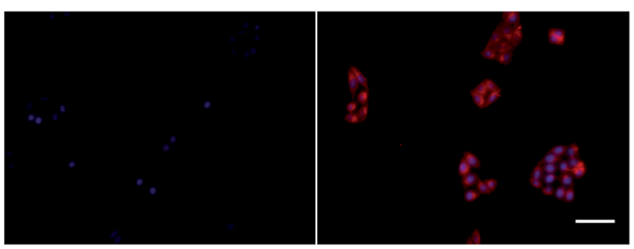

Fig. 8 Fluorescence images of fixed HeLa Kyoto cells incubated with **CNO-1b** at pH 8.5 (left), and 4.5 (right). Nuclei stained blue with DAPI. Imaged at 20× magnification. (Scale bar 100 μm).

retained its ability to turn fluorescence off and on intracellularly, the pH of two imaging wells was adjusted to 8.5 and 4.5 and re-imaged. Gratifyingly, a strong NIR emission intensity was clearly seen in the cells at pH 4.5 (Fig. 8, right) when compared to a weak trace NIR emission at pH 8.5 (Fig. 8, left). Confocal *z*-stacks of cells containing **CNO-1b** confirmed that the CNOs were internalized by the cell.

Conclusions

In summary, boron difluoride azadipyrromethene functionalized CNO conjugates have been synthesised and characterised. The NIR fluorescence properties of the difluoride azadipyrromethenes are retained after covalent linking to the CNO, allowing intracellular identification with LSCM imaging. The ability to reversibly switch on and off the NIR fluorescence by the pH controlled phenol/phenolate modulation of the fluorophore linked CNOs was demonstrated both in solution and *in vitro*. This ability to report on environmental changes *in vitro* offers significant scope for the development of smart responsive CNO constructs. Further surface functionalization of the CNOs is ongoing to allow the incorporation of targeting moieties as well as for drug delivery systems, potentially leading to tailor-made theranostic nanomaterials.

Acknowledgements

The authors wish to thank Adrian Villalta-Cerdas (University of Texas at El Paso) for CNO synthesis, Giammarino Pugliese (IIT) for TGA measurements, Nicola Pesenti for AFM and Rosaria Brescia (IIT) for HRTEM. Istituto Italiano di Tecnologia and Science Foundation Ireland are greatly acknowledged for research funding. We also thank the Department of Nanochemistry at IIT for cell culture facility. DW thanks China Scholarship Council for a Ph.D. fellowship. LE would like to thank the US NSF, PREM Program (DMR-1205302) and the Robert A. Welch Foundation (Grant AH-0033) for generous support.

Notes and references

1 C. Fabbro, H. Ali-Boucetta, T. Da Ros, K. Kostarelos, A. Bianco and M. Prato, *Chem. Commun.*, 2012, **48**, 3911–3926.
2 B. S. Wong, S. L. Yoong, A. Jagusiak, T. Panczyk, H. K. Ho, W. H. Ang and G. Pastorin, *Adv. Drug Delivery Rev.*, 2013, **65**, 1964–2015.
3 D. Ugarte, *Nature*, 1992, **359**, 707–709.
4 D. Ugarte, *Carbon*, 1995, **33**, 989–993.
5 J. L. Delgado, M. A. Herranz and N. Martin, *J. Mater. Chem.*, 2008, **18**, 1417–1426.
6 A. Molina-Ontoria, M. N. Chaur, M. E. Plonska-Brzezinska and L. Echegoyen, *Chem. Commun.*, 2013, **49**, 2406–2408.
7 L. Ding, J. Stilwell, T. Zhang, O. Elboudwarej, H. Jiang, J. P. Selegue, P. A. Cooke, J. W. Gray and F. F. Chen, *Nano Lett.*, 2005, **5**, 2448–2464.
8 M. Yang, K. Flavin, I. Kopf, G. Radics, C. H. A. Hearnden, G. J. McManus, B. Moran, A. Villalta-Cerdas, L. A. Echegoyen, S. Giordani and E. C. Lavelle, *Small*, 2013, **9**, 4194–4206.
9 R. Wang and F. Zhang, *J. Mater. Chem. B*, 2014, **2**, 2422–2443.
10 A. Palma, L. A. Alvarez, D. Scholz, D. O. Frimannsson, M. Grossi, S. J. Quinn and D. F. O'Shea, *J. Am. Chem. Soc.*, 2011, **133**, 19618–19621.
11 M. Ghosh, S. K. Sonkar, M. Saxena and S. Sarkar, *Small*, 2011, **7**, 3170–3177.
12 S. K. Sonkar, M. Ghosh, M. Roy, A. Begum and S. Sarkar, *Mater. Express*, 2012, **2**, 105–114.
13 D. O. Frimannsson, M. Grossi, J. Murtagh, F. Paradisi and D. F. O'Shea, *J. Med. Chem.*, 2010, **53**, 7337–7343.
14 D. Wu and D. F. O'Shea, *Org. Lett.*, 2013, **15**, 3392–3395.
15 P. Batat, M. Cantuel, H. Jonusauskas, L. Scarpantonio, A. Palma, D. F. O'Shea and N. D. McClenaghan, *J. Phys. Chem. A*, 2011, **115**, 14034–14039.
16 A. Palma, M. Tasior, D. O. Frimannsson, T. T. Vu, R. Méallet-Renault and D. F. O'Shea, *Org. Lett.*, 2009, **11**, 3638–3641.
17 J. Murtagh, D. O. Frimannsson and D. F. O'Shea, *Org. Lett.*, 2009, **11**, 5386–5389.
18 M. Yuan, X. Yin, H. Zheng, C. Ouyang, Z. Zuo, H. Liu and Y. Li, *Chem.–Asian J.*, 2009, **4**, 707–713.
19 S. Y. Leblebici, L. Catane, D. E. Barclay, T. Olson, T. L. Chen and B. Ma, *ACS Appl. Mater. Interfaces*, 2011, **3**, 4469–4474.
20 A. N. Amin, M. E. El-Khouly, N. K. Subbaiyan, M. E. Zandler, S. Fukuzumi and F. D'Souza, *Chem. Commun.*, 2012, **48**, 206–208.
21 V. Bandi, K. Ohkubo, S. Fukuzumi and F. D'Souza, *Chem. Commun.*, 2013, **49**, 2867–2869.
22 V. Bandi, M. E. El-Khouly, K. Ohkubo, V. N. Nesterov, M. E. Zandler, S. Fukuzumi and F. D'Souza, *J. Phys. Chem. C*, 2014, **118**, 2321–2332.
23 K. Flavin, K. Lawrence, J. Bartelmess, M. Tasior, C. Navio, C. Bittencourt, D. F. O'Shea, D. M. Guldi and S. Giordani, *ACS Nano*, 2011, **5**, 1198–1206.
24 K. Flavin, I. Kopf, J. Murtagh, M. Grossi, D. F. O'Shea and S. Giordani, *Supramol. Chem.*, 2011, **24**, 23–28.
25 S. O. McDonnell, M. J. Hall, L. T. Allen, A. Byrne, W. M. Gallagher and D. F. O'Shea, *J. Am. Chem. Soc.*, 2005, **127**, 16360–16361.
26 K. Flavin, M. N. Chaur, L. Echegoyen and S. Giordani, *Org. Lett.*, 2009, **12**, 840–843.
27 C. T. Cioffi, A. Palkar, F. Melin, A. Kumbhar, L. Echegoyen, M. Melle-Franco, F. Zerbetto, G. M. A. Rahman, C. Ehli, V. Sgobba, D. M. Guldi and M. Prato, *Chem.–Eur. J.*, 2009, **15**, 4419–4427.
28 V. V. Didenko, V. C. Moore, D. S. Baskin and R. E. Smalley, *Nano Lett.*, 2005, **5**, 1563–1567.
29 B. Tian, C. Wang, S. Zhang, L. Feng and Z. Liu, *ACS Nano*, 2011, **5**, 7000–7009.
30 Y. Liu, C.-y. Liu and Y. Liu, *Appl. Surf. Sci.*, 2011, **257**, 5513–5518.